Small and Large Radicals in Thin-Film Polymer Depolymerization

Roland E. Florin and Leo A. Wall*

Polymer Chemistry Section, National Bureau of Standards, Washington, D. C. 20234.
Received March 31, 1970

ABSTRACT: Rates of polymer decomposition are enhanced or retarded as a result of the escape of small free radical or other species through the surface of thin films. Solutions for the rate equations are given as a function of thickness for a mechanism involving the competitive diffusion of small and large radicals. The enhancement of the rates of depolymerization of polytetrafluoroethylene observed with thin films is explained by the model. Comparison of the experimental results with theory indicates that the irradiation of polytetrafluoroethylene produces comparable amounts of both large and small radicals. The mechanisms discussed are undoubtedly operative in many other situations involving the radiolysis or pyrolysis of polymers, for example, the radiation-induced cross-linking of polymers.

In large samples it is obvious that sample dimensions can influence the decomposition of polymers by way of retarded monomer escape, or of heat transfer restrictions. Some possible causes of sample size or surface influence have been put forward[1-3] in the past. We have found evidence for another mechanism for dimensional effects on rates which is operative at considerably smaller sample size, and which should be of general importance. The basic feature is that in cases where both large and small radicals or other small species participate in the reaction, the latter can escape at the surface, thus modifying the steady-state concentrations of all radicals in the shallower layers, and in particular that of the decomposing polymer radicals. In earlier studies of the trapping of small radicals at 4°K, it was observed that the radiolysis of solid methane produced methyl radicals and hydrogen atoms of different concentrations[4] at long times. A theoretical treatment[4] of this situation required consideration of the competitive diffusion of the two species.

The specific process treated here is that of the radiation-induced decomposition of polytetrafluoroethylene at 400–450°. It will be shown that the back-reaction of monomer is inadequate to explain the observed trend of decomposition rate as a function of sample thickness,[5] while the proposed mechanism of altered radical concentrations successfully does so.

Inadequacy of Back-Reaction Mechanism. The data discussed are chiefly those reported previously[5] in which polytetrafluoroethylene was decomposed under flowing helium, at temperatures of 400–450° and ^{60}Co γ dose rates of 0.1–7.66 Mrad/hr. In Figure 1 the original measurements of the radiation-induced increment in rate of decomposition to volatiles have been reduced to plots of overall rates of decomposition in per cent per minute as a function of sample thickness, at constant dose rate and temperature. The logarithmic plots in Figure 1 are concave upward and disagree with the curvature deduced[5] from the mechanism involving retarded monomer escape and back-reaction (Figure 1, dashed line).

Kinetic Model with Diffusion. Background. The free-radical chain theory of polymer decomposition is assumed together with the knowledge that in polytetrafluoroethylene the rate of monomer production is essentially that of the overall decomposition. In the radiation-induced decomposition, the occurrence of F atoms or products derived from them is implied by observation of their congener, the side-chain radical[6] $\sim\!\!\sim CF_2\dot{C}FCF_2\sim\!\!\sim$. These probably result from the process

$$\sim\!\!\sim CF_2CF_2CF_2\sim\!\!\sim \xrightarrow{\gamma} \sim\!\!\sim CF_2\dot{C}FCF_2\sim\!\!\sim + F$$

It is not important to the argument whether F atoms persist as such or perhaps add to monomer to form other small radicals

$$F + C_2F_4 \longrightarrow C_2F_5$$

In a fluorocarbon system neither the F atom nor the C_2F_5 radical is likely to abstract and their principal fate must be termination with each other or with large radicals, or evaporation from surface layers. A survey of relative diffusion rates of polymeric molecules and small molecules, approximately $1\text{–}10 \times 10^{-7}$ and 1×10^{-5} $cm^2\ sec^{-1}$, respectively,[7-9] suggests that it is permissible to neglect the migration of polymeric radicals. Relative termination rates are involved in the theory as well. Many of the known termination rate constants for small plus small[8-10] and large plus large[8,9,11,12] radicals are in the range $1\text{–}6 \times 10^9$ and $0.2\text{–}7 \times 10^7$ l. mol^{-1} sec^{-1}, respectively. It must be cautioned that all these values are for dilute solution near room temperature, while the medium under discussion is molten polymer at several

* To whom correspondence should be addressed.

(1) L. A. Wall, L. J. Fetters, and S. Straus, *Polym. Lett.*, **5**, 721 (1967).
(2) H. H. G. Jellinek and H. Kachi, *Polym. Eng. Sci.*, **5**, 1 (1965).
(3) S. Straus and L. A. Wall, *J. Res. Nat. Bur. Stand., Sect. A*, **65**, 223 (1961).
(4) D. W. Brown, R. E. Florin, and L. A. Wall, *J. Phys. Chem.*, **66**, 2602 (1962).
(5) R. E. Florin, M. S. Parker, and L. A. Wall, *J. Res. Nat. Bur. Stand., Sect. A*, **70**, 115 (1966).
(6) H. N. Rexroad and W. Gordy, *J. Chem. Phys.*, **30**, 399 (1959).
(7) G. Meyerhoff and G. V. Schulz, *Makromol. Chem.*, **7**, 294 (1952); P. J. Flory, "Principles of Polymer Chemistry," Cornell University Press, Ithaca, N.Y., 1953, p 306.
(8) P. E. M. Allen and C. R. Patrick, *Makromol. Chem.*, **48**, 89 (1961).
(9) P. E. M. Allen and C. R. Patrick, *ibid.*, **72**, 106 (1964).
(10) M. Anbar and P. Neta, *Int. J. Appl. Radiat. Isotop.*, **16**, 227 (1965).
(11) A. M. North, "The Collision Theory of Chemical Reactions in Liquids," Methuen, London, 1964, p 132.
(12) G. M. Burnett, "Mechanism of Polymer Reactions," Interscience, New York, N. Y., 1954, p 384.

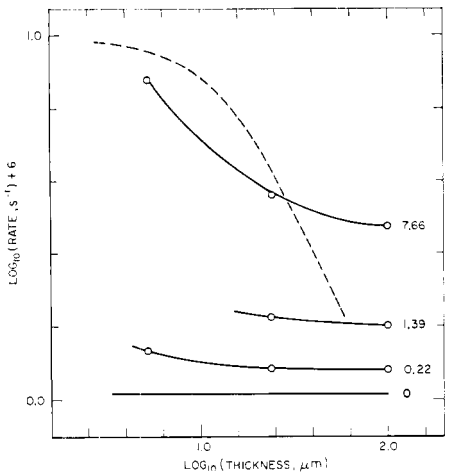

Figure 1. γ-Ray-induced depolymerization of polytetrafluoroethylene at 430°, full lines observed rates of monomer production as a function of sample thickness. Numbers to right of curves are dose rates, Mrad/hr. Dashed line is theory for reverse propagation mechanism.[5]

hundred degrees Celsius. Wider ranges of variation are suggested by values of diffusivity of small molecules in elastomers, of the order of 10^{-6} and 10^{-7} cm^2 sec^{-1},[13] and by one termination constant 4.0×10^4 l. mol^{-1} sec^{-1} determined in a decomposing polymer melt.[12] As a hypothesis concerning large plus small termination rates we rely on a formulation given originally in Smoluchowski's diffusion theory for spherical molecules, but often accepted in more complicated cases as well[8,9] (eq 1a). Here k_{12} represents the rate constant for the

$$k_{12} = \frac{4\pi N_0}{1000}(D_1 + D_2)r_{12} \qquad (1a)$$

reaction of small with large molecules, N_0 is the Avogrado number, D_1 and D_2 are diffusivities, and r_{12} is the encounter distance in centimeters. Units of k_{12} in eq 1a are l. mol^{-1} sec^{-1}.

It is likely that for actual small molecules relative to large polymeric molecules, the encounter distances are essentially identical, and diffusivities are greatly different. Thus, setting $r_{12} = r_{11}$ and $D_2 \ll D_1$, eq 1b follows

$$k_{12} \cong \frac{1}{2}k_{11} \qquad (1b)$$

from eq 1a, where k_{11} is the rate constant for reaction of two small molecules.

The above amounts to the estimate that large plus small termination rate constants are of the same order of magnitude as small plus small, and roughly about half as great. Polymeric radicals thus terminate with each other slowly, while small radicals terminate with each other or with large radicals much more rapidly. In layers near the surface, small radicals are depleted and only the slow termination of large plus large radicals remains. There is thus a high surface concentration of large radicals and a consequent high surface rate of decomposition. These considerations are embodied in Table I, where only random initiations are considered.

(13) V. Stannett, "Diffusion in Polymers," J. Crank and G. S. Park, Ed., Academic Press, New York, N. Y., 1968, pp 47–50.

TABLE I

Reaction	Rate
P → R	v_1, or $k_1\rho m + \Phi_1 I\rho/m$
P → S	v_2, or $\Phi_2 I\rho/m$
$R_{j+2} \rightarrow R_j$ + monomer	k_2R
R + R → P	k_4R^2
R + S → RS	k_5RS
S + S → products	k_6S^2

Interesting special cases containing thermolytic end initiation can be developed, and at least one such will be mentioned later in this article.

Six reactions appear in the table, but the propagation, k_2R, is involved only perfunctorily. P, R, and S refer to polymer segments, polymer radicals, and small radicals, respectively. The symbols v_1 and v_2 are radical generation rates; the alternative expressions given involve a random thermal initiation rate constant k_1, density ρ, segment molecular weight m, radiation dose rate I, and radiation efficiency factors Φ_1 and Φ_2. Because the small radical diffusivity D, cm^2 sec^{-1}, will be used, concentration and rate-constant units are in moles, cubic centimeters, and seconds.

We consider the time-independent steady state in a strip sample of thickness X (centimeters) with position-variable x (centimeters) below the free surface and an impermeable bottom. Evaporation of small radicals S keeps a surface concentration, $S = 0$, at $x = 0$. The steady state with diffusion is then

$$\frac{dS}{dt} = 0 = v_2 - k_6S^2 - k_5RS + D\frac{d^2S}{dx^2} \qquad (2)$$

$$\frac{dR}{dt} = 0 = v_1 - k_4R^2 - k_5RS \qquad (3)$$

Solutions of Equations. The solution for concentration as a function of depth is a relatively simple quadrature in dimensionless quantities, the derivation of which is tedious but straightforward (Appendix I)

$$\xi = \int_{y_1}^{y_2} (1 + y^{-2})\{C + {}^1/_3(1 - L^{-2})y^3 + (M + L^{-2})y + (1 - M - L^{-2})y^{-1} + {}^1/_3L^{-2}y^{-3}\}^{-1/2}\,dy \qquad (4)$$

where C is an integration constant determined by the boundary conditions. The dimensionless quantities are defined for this and subsequent relationships

$$y = R(k_4/v_1)^{1/2}$$

$$L = k_5(k_4k_6)^{-1/2}$$

$$M = v_2/v_1$$

$$\xi = x\left(\frac{2L}{D}\right)^{1/2}(v_1k_6)^{1/4}$$

$$\xi_0 = X\left(\frac{2L}{D}\right)^{1/2}(v_1k_6)^{1/4}$$

$$Z = k_4R^2m/k_1\rho$$

$$w = k_4R^2m/\Phi_1I\rho$$

$$f = \Phi_1I/k_1,\ h = \Phi_2/\Phi_1,\ b = 1/(L^2 - 1)$$

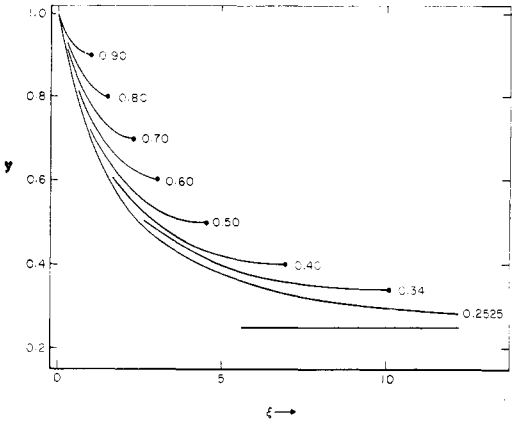

Figure 2. Radical concentration profiles in strips of various thicknesses, eq 4: ordinates, dimensionless large-radical concentration parameter y; abscissae, dimensionless depth parameter ξ; numbers on curves, y_0 value; ●, indicates bottom of strip (y_0, ξ_0); curve 0.2525, and horizontal line, infinitely thick strip and threshold y; $L = 31.6$, $M = 0.95$.

The properties of eq 4 are shown in Figures 2 and 3 where the local steady state value of the dimensionless concentration parameter, y, is plotted as a function of the depth parameter, ξ, for various values of the generation ratio, M, and termination ratio, L. Within a given family, the curve for threshold concentration, y_0, corresponding to infinite thickness, is a limiting case, from which the others depart earlier than the lower the thickness. The $M = 0.95$ curves of Figure 2 require a longer ξ interval than do the lower value $M = 0.5$ and $M = 0.8$ to approach the thick-film limiting concentration. This interval is lengthened extremely if $M = 1$.

For expressions proportional to the rate per unit weight or volume, assuming as before that the whole weight loss rate goes as $dM/dt = k_2R$, one needs the average

$$\bar{y} = \int_0^{\xi_0} y\,d\xi \Big/ \int_0^{\xi_0} d\xi = \int_1^{y_0} y\frac{d\xi}{dy}dy \Big/ \int_1^{y_0} \frac{d\xi}{dy}dy \quad (5)$$

where y_0 is the value of y at the bottom of the sample. Numerical evaluation involves no new quantities beyond eq 4. Figure 4 shows logarithmic curves of the scaled average rate $\bar{y}$ as a function of the scaled thickness ξ_0, for choices of L and M which seemed reasonable in

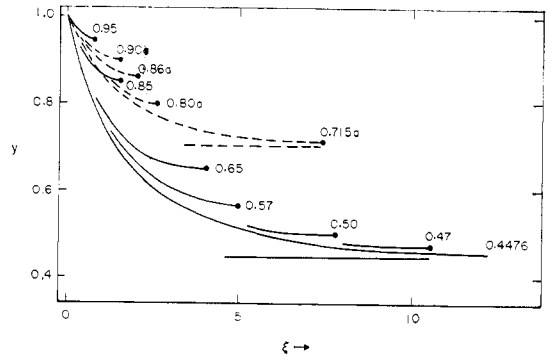

Figure 3. Radical concentration profiles in strips of various thicknesses, eq 4. Coordinates as in Figure 2; cases $L = 100$, $M = 0.5$ (. . ., suffix a), and $L = 100$, $M = 0.8$ (——); horizontal lines, threshold y values; curve 0.4476, infinitely thick strip.

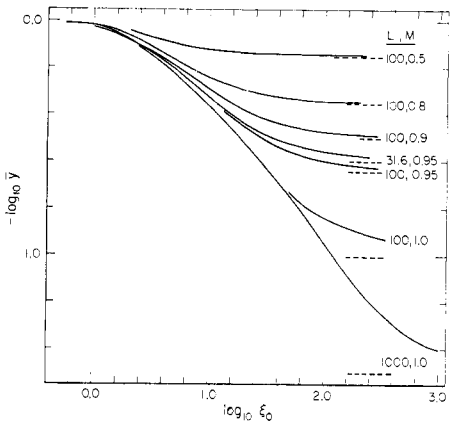

Figure 4. Theoretical rates of monomer production as a function of sample thickness, eq 4. Pairs of numbers at right are values for the parameters L, M; horizontal dashed lines give limiting rate value, y, at infinite thickness.

the light of known diffusion and rate constants and initial comparison with experiment. The basis of choice has been discussed in part in the beginning of this article. Comments on numerical and graphical handling appear in Appendix II. It can be seen from Figure 4 that over a wide range of L the course of the curves depends upon M more than on L. For mixed thermal and radiation initiation, M, the ratio of generation rates of small *vs.* large radicals, will vary with dose rate. The change of the average rate with thickness is, of course, slower than the change of local rate with depth, because of the distribution among all layers, but seems substantially complete in a thickness range of 100- to 1000-fold.

Comparison with Experiment. Comparison with experiment is rather indirect and we have relied on successive trials. Possible values of L and M within the tolerance of the data are easily enough found by sliding theoretical curves, Figure 4, over the experimental points, Figure 1. The displacements of axes needed to secure a match furnish further parameters. A permissible set of curves for different dose rates is further restricted by the relation of M to dose rate

$$M = \Phi_2 I/(k_1 + \Phi_1 I)$$

A fair match between Figure 4 and the 7.66-Mrad curve of Figure 1 is given by $L = 100$, $M = 1$, $\log(\xi_0/X) = 4.66$, $\log(y/\text{rate}) = +4.6$. Poorer matches, perhaps within the limits of error, are given by $L = 31.6$ or 100, $M = 0.95$, $\log(\xi/X) = 4.50$, $\log(y/\text{rate}) = 4.87$. Using the relation

$$\log\left(\frac{\xi_0}{X}\right) = \log\left(\frac{2L}{D}\right)^{1/2}\left[\frac{\rho}{m}(k_1 + \Phi_1 I)k_6\right]^{1/4}$$

we substitute the last-mentioned log shift value $\log(\xi_0/X) = 4.50$, the plausible values $D = 10^{-5}$ cm^2 sec^{-1} and $k_6 = 10^{13}$ cm^3 sec^{-1}, and, from ref 5, $\rho/m = 0.01438$ mol/cm^3, $\Phi_1 = 3.64 \times 10^{-8}$ sec^{-1} Mrad^{-1} hr, k_1 at 429.5° $= 2.28 \times 10^{-8}$ sec^{-1}, and leave L to be determined. The result is $L = 80$. Also, in the relation

$$\log\left(\frac{y}{\text{rate}}\right) + 2\log\left(\frac{\xi_0}{X}\right) = \log\left(\frac{2k_5\rho}{k_2 D m}\right)$$

the same substitutions and log (y/rate) = 4.87, $2k_5$ = 10^{13} cm^3/mol sec, yield log k_2 = 2.13. If A_2 = 10^{13} sec^{-1}, this involves at 429.5°, E_2 = 35.2 kcal, a possible value. More critical comparisons would require much more accurate data.

The present account of rate variations with thickness in radiation-induced depolymerization implies a somewhat larger kinetic chain or zip length for the thermal depolymerization than estimated earlier.[5] This dose not interfere with any earlier deductions as to the mechanism of the thermal depolymerizations. The observed radical yield, $G(R)$ = 3, and the measured efficiency factor, Φ = 3.64 × 10^{-8} sec^{-1} Mrad^{-1} hr, determined there are identifiable with the present Φ_1. In the kinetic equations, however, Φ should be replaced by Φ_1 in the thin-film limit, but by $\Phi_1 - \Phi_2$ approximately in the thick-film limit, and, in between, by a fractional value which varies slowly with dose rate. The shapes in Figures 1 and 4 suggest that the 0.0025-cm films of ref 5 are nearer to the thick-film than to the thin-film limit. As Φ_2/Φ_1 must be fairly near to 1 to satisfy the M = 0.95 match, the changes involve lowering the estimate of k_1 and thus raising the kinetic chain length for pure thermal decomposition by a factor perhaps as great as fivefold. The values Φ_2/Φ_1 = 1 and M = 1, precisely, are special cases.

When Φ_2/Φ_1 = 1, precisely, the simplified interpretation just given still applies to the thin film but not to the thick. The M = 1 curves also have abnormal properties, as seen in Figure 4, notably the greater sensitivity to L values and the great difference between behavior of thick and thin films.

The Limit of Infinite Depth. The limiting state at infinite depth is of some interest in choosing limits of integration, and also in its own right in more complicated cases of radiation-induced decomposition. Equations 2 and 3, with $d^2S/dx^2 = 0$, lead to the relations

$$Z^2 + Z[-(1 + f)(1 - b) + hf(1 + b)] - b(1 + f)^2 = 0 \quad (6)$$

for mixed initiation and

$$w^2 + w(-1 + h + b + bh) - b = 0 \quad (7)$$

for initiation exclusively by radiation. Symbols are defined under eq 4. For pure radiation initiation, the ratio $w = k_4R^2m/\Phi_1I\rho$ is independent of dose rate I, and so, in our situation of rate proportional to k_2R, R and rate are proportional to the square root of I even though two radical species interact. In mixed initiation, Z or R^2 *vs.* I describes a hyperbola with oblique axes. Here R^2 is no longer linear in I as in ref 5, and the methods of isolation of parameters described there will fail. Nevertheless, if b is small and h not too close to 1, as would be satisfied for $L > 10$, $\Phi_2/\Phi_1 < 0.95$, a crude approximation to the solution of eq 6 at moderate dose rates is $Z = 1 + (1 - h)f$ or

$$R_{\text{interior}}{}^2 \doteq \frac{k_1\rho}{k_4m} + \frac{(\Phi_1 - \Phi_2)\rho}{k_4m} I$$

Thus, the condition for the treatment of ref 5 remains as a crude approximation with modified parameters, unless $\Phi_2 = \Phi$.

General Discussion

Other Applications. It is at first surprising that the present mechanism has a transition from thin-film to thick-film behavior at thicknesses much less than those involved in retarded monomer escape. The latter experimentally appears to cause no change of regime until thicknesses of tenths of a millimeter,[14] under roughly comparable conditions. Superficially, this difference in location of the transition region can be rationalized by noting that although the diffusivities, D, may be similar for monomer and small radicals, S, *e.g.*, 10^{-5} cm^2 sec^{-1}, the pertinent concentrations are very much smaller for the radicals. This suggests, by the inversion of Fick's first law

$$\frac{dC}{dx} = \left(\frac{1}{D}\right)(\text{flux rate})$$

that at similar flux rates the radicals can go from near zero to near their maximum permissible concentration over a shorter interval. The full truth is not so simple, and would require comparison of generation and destruction rates as well. Although our treatment was developed in order to elucidate γ-ray-induced depolymerizations, it would be expected to apply to thermal depolymerizations initiated at the ends of polymer molecules depending on the size and diffusivity of the small radical produced.

Polystyrene[15] is thought to initiate with production of small radicals; however, it also has a very short kinetic chain length and hence the effect would probably be very difficult to detect.

Essentially, the same mechanism can conceivably lead to slower rates with thinner films. Consider the following types of pseudomonomolecular termination processes

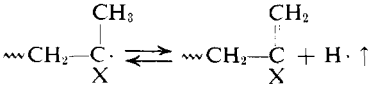

or

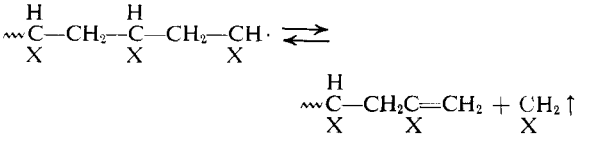

which would operate most efficiently at the surface of decomposing polymer melt or film. Thus, diffusion situations between large and small radicals or molecular species are likely to produce larger or smaller rates in thermolysis or radiolysis of small thin samples of polymeric materials.

However, when the modes of initiation and termination just discussed exist together and are equally affected by diffusion, the net result of changes in thickness is merely a change of kinetic chain length with no change in rate. To illustrate, let the steps be designated as

Initiation

$$Q \xrightarrow{k_1} R + S$$

(14) J. C. Siegle, L. T. Muus, Tung-Po Lin, and H. A. Larsen, *J. Polym. Sci., Part A*, **2**, 391 (1964).

(15) G. G. Cameron, *Makromol. Chem.*, **100**, 260 (1967).

Propagation

$$R_{j+2} \xrightarrow{k_2} R_j + M$$

Termination

$$R \xrightarrow{k_4} Q + S$$

where Q, M, R, and S denote polymer molecules, monomer, large radicals, and small radicals, and let the net effect of reduction in thickness be to double k_1 and k_4. Then the rate k_2R is unchanged

$$k_2R = \frac{k_2k_1Q}{k_4}$$

while the kinetic chain length l is reduced to one-half

$$l = \frac{k_2R}{k_4R} = \frac{k_2}{k_4}$$

Some of these effects of thickness may have been encountered in other polymers. Films of poly(methyl methacrylate) studied by Robb[16] gave higher rates at such small thicknesses, 40 nm, that the mechanism treated here could be expected there as well. Their results in view of the high temperatures, short times, and procedures used, suggest in our opinion many other possible explanations.

Qualitatively, the interaction of large and small radicals at various depths could be important in still other reactions. The cosmic dust particles discussed by Donn,[17] containing hydrocarbon and exposed to ultraviolet, are small enough, 1–10 nm thickness, so that efficient escape of H atoms would occur from a large portion or all of a particle. The radiation cross-linking of crystalline polyethylene is known to depend on thickness,[18] as follows readily from our analysis if unescaped H atoms scavenge polymer radicals which would otherwise combine as cross-links. The mechanistic consequences of diffusion and thickness would also be of obvious importance in oxidative degradation. These situations will not be included in this article.

Appendix I

Solution of Radical Concentration Equations

$$\begin{cases} \frac{dS}{dt} = 0 = v_2 - k_6S^2 - k_5RS + D\frac{d^2S}{dx^2} & (2) \\ \frac{dR}{dt} = 0 = v_1 - k_4R^2 - k_5RS & (3) \end{cases}$$

Introducing the dimensionless quantities, M, y, S', and L, which are defined by the relations

$$v_2 = Mv_1,\ R = y\left(\frac{v_1}{k_4}\right)^{1/2},\ S = S'\left(\frac{Mv_1}{k_6}\right)^{1/2}$$

$$k_5 = L(k_4k_6)^{1/2}$$

eq 2 and 3 then become

$$\begin{cases} 1 - S'^2 - LM^{-1/2}yS' + D(Mv_1k_6)^{-1/2}\frac{d^2S'}{dx^2} = 0 & (8) \\ 1 - y^2 - LM^{1/2}yS' = 0 & (9) \end{cases}$$

Equation 9 is then rearranged to give

$$S' = \frac{1}{LM^{1/2}}\left(\frac{1}{y} - y\right) \quad (10)$$

which, upon double differentiation, becomes

$$\frac{d^2S'}{dx^2} = \frac{1}{LM^{1/2}}\left[\frac{2}{y^3}\left(\frac{dy}{dx}\right)^2 - \frac{1+y^2}{y^2}\left(\frac{d^2y}{dx^2}\right)\right] \quad (11)$$

The limit for the infinite interior is considered first. Setting $d^2S'/dx^2 = 0$, eq 8 and 9 give

$$(L^2 - 1)y^4 + [L^2M - L^2 + 2]y^2 - 1 = 0 \quad (12)$$

which is the solution for y at the interior of an infinitely thick sample. Equation 12 can be subdivided into two cases.

The first is pure radiation initiation, in which case

$$v_2 = \Phi_2I\frac{\rho}{m},\ v_1 = \Phi_1I\frac{\rho}{m}$$

and hence $M = \Phi_2/\Phi_1$, independent of dose rate. The solution for

$$y^2 \equiv R^2\frac{k_4}{v_1} = \frac{R^2k_4}{\Phi_1I}$$

is also a constant independent of I; thus, $R = C\sqrt{I}$, where $C^2 = \Phi_1/k_4$ times the root of the quadratic (12) in y^2. The result is expressed also in eq 7.

The second is mixed initiation, in which case

$$v_1 = k_1\frac{\rho}{m} + \Phi_1I\frac{\rho}{m}$$

$$v_2 = \Phi_2I\frac{\rho}{m}$$

Then quantities f, h, and Z are given by

$$f = \frac{\Phi_1I}{k_1}$$

$$h = \frac{\Phi_2}{\Phi_1}$$

and

$$Z = y^2(1+f) = \frac{k_4R^2m}{k_1\rho}$$

and eq 12 now becomes

$$(L^2 - 1)\frac{Z^2}{(1+f)^2} + \left[L^2\frac{hf}{1+f} - L^2 + 2\right]\frac{Z}{1+f} - 1 = 0 \quad (13)$$

This rearranges to eq 6, which is second degree in Z and f, and therefore also in R^2 and I.

The discriminant and a numerical plot show that eq 6 is a hyperbola in the $Z - f$ space having symmetric axes skewed with respect to the coordinate axes.

The equation for a finite thickness is obtained by substituting eq 10 and 11 in eq 8, to give

(16) A. Barlow, R. S. Lehrle, and J. C. Robb, *Makromol. Chem.*, **54**, 230 (1962).

(17) B. Donn, "Formation and Trapping of Free Radicals," A. M. Bass and H. P. Broida, Ed., Academic Press, New York, N. Y., 1960, p 347.

(18) R. Salovey and M. Y. Hellman, *Polym. Prepr., Amer. Chem. Soc., Div. Polym. Chem.*, **9**, 1124 (1968).

$$1 - \frac{(1-y)^2}{L^2My^2} - \frac{1-y^2}{M} + \frac{D}{LM(v_1k_6)^{1/2}}\left[\frac{2}{y^3}\left(\frac{dy}{dx}\right)^2 - \frac{1+y^2}{y^2}\left(\frac{d^2y}{dx^2}\right)\right] = 0 \quad (14)$$

Upon multiplying by

$$\frac{LM(v_1k_6)^{1/2}y^2}{D(1+y^2)}$$

we obtain

$$\frac{d^2y}{dx^2} - \frac{2}{y(1+y^2)}\left(\frac{dy}{dx}\right)^2 = K'\frac{y^2}{1+y^2}\left[1 - \frac{(1-y^2)^2}{L^2My^2} - \frac{1-y^2}{M}\right] \quad (15)$$

where

$$K' = \frac{LM(v_1k_6)^{1/2}}{D}$$

Let

$$p = \frac{dy}{dx}, \quad \frac{d^2y}{dx^2} = p\frac{dp}{dy} = {}^1/_2\frac{d(p^2)}{dy}$$

Double coefficients and eq 15 becomes linear first order in p^2

$$\frac{d(p^2)}{dy} + Pp^2 = Q$$

for which the general solution is well known; namely

$$p^2 = e^{-\int P dy}\left\{C' + \int e^{\int P dy} Q dy\right\}$$

where C' is an integration constant. Since

$$P = -\frac{4}{y(1+y^2)}$$

$$\int P dy = -4 \ln y + 2 \ln(1+y^2)$$

$$e^{\int P dy} = \frac{(1+y^2)^2}{y^4}$$

thus

$$p^2 \equiv \left(\frac{dy}{dx}\right)^2 = \frac{y^4}{(1+y^2)^2}\left\{C' + \int\frac{(1+y^2)^2}{y^4}2K'\frac{y^2}{1+y^2}\left[1 - \frac{(1-y^2)^2}{L^2My^2} - \frac{1-y^2}{M}\right]dy\right\} \quad (16)$$

The integrand is reduced to

$$\frac{2K'}{L_2M}\left[(L^2-1)y^2 + (L^2M+1) + (L^2M - L^2 + 1)\frac{1}{y^2} - \frac{1}{y^4}\right]$$

which integrates to

$$\frac{2K'}{L^2M}\left[\frac{(L^2-1)y^3}{3} + (L^2M+1)y + (L^2 - L^2M - 1)\frac{1}{y} + \frac{1}{3y^3}\right]$$

Consolidating constants, reducing, and inverting, we now obtain for $1/p$

$$\frac{dx}{dy} = \frac{1+y^2}{y^2}\left(\frac{M}{2K'}\right)^{1/2}\left\{C + \frac{1-L^{-2}}{3}y^3 + (M + L^{-2})y + (1 - M - L^{-2})\frac{1}{y} + \frac{1}{3L^2y^3}\right\}^{-1/2} \quad (17)$$

Replacing X by ξ, by using the relation

$$\xi = x\left(\frac{2L}{D}\right)^{1/2}\left(v_1k_6\right)^{1/4}$$

and integrating, eq 4 is obtained.

Appendix II

Numerical Integrations. Integration constants C and lower boundary concentration numbers of y_0 for eq 4 are obtained in pairs by using the condition

$$\frac{dy}{d\xi} = 0$$

It is sufficient to set equal to zero the radicand of eq 4. At infinite thickness the choice of y_0 is given by eq 12, 6, or 7. Computations were done on a desk electronic computer capable of handling square roots, with tabulation of y, $d\xi/dy$, $y(d\xi/dy)$, and the integral increments $\Delta\xi$ and $\Delta(\int y d\xi)$. The latter were mostly obtained by Simpson's rule. Near y_0, where the integrand becomes infinite, there are intermediate and end regions where the approximations

$$\left(\frac{d\xi}{dy}\right)^{-1} = my + b \quad (18)$$

and

$$\left(\frac{d\xi}{dy}\right)^{-2} = my + b \quad (19)$$

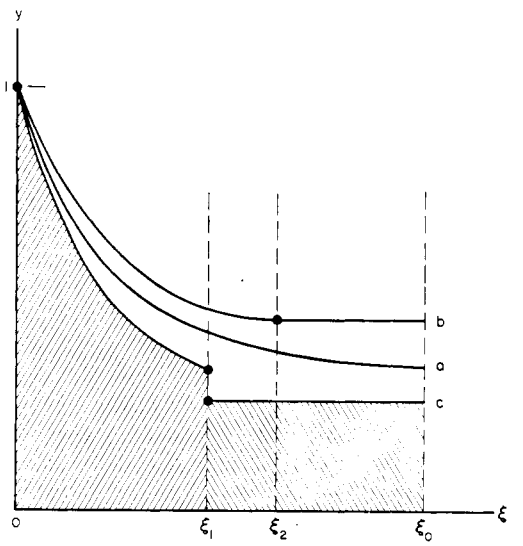

Figure 5. Boundary conditions used for various numerical integrations of eq 4, see Appendix II: a, actual solution to be approximated; b, numerical integration carried to depth ξ_2 for finite sample thickness and continued to center at same value; c, numerical integration carried to depth ξ_1 for infinitely thick sample and continued at value for infinite depth.

respectively, hold satisfactorily. Here the numerical formulas used were

$$\xi_i - \xi_j = \frac{y_i - y_j}{\left(\frac{d\xi}{dy}\right)_i^{-1} - \left(\frac{d\xi}{dy}\right)_j^{-1}} \ln \frac{\left(\frac{d\xi}{dy}\right)_i}{\left(\frac{d\xi}{dy}\right)_j} \quad (20)$$

and

$$\xi_i - \xi_j = \frac{2(y_i - y_j)}{\left(\frac{d\xi}{dy}\right)_i^{-1} - \left(\frac{d\xi}{dy}\right)_j^{-1}} \quad (21)$$

If y_0 and C are near the infinite-thickness values, intervals must be shortened as y_0 is approached. In the thickest finite range, bounds for $\bar{y}(\xi_0)$ are

$$y_u + \xi_0^{-1}[I_2(\xi_1) - y_u\xi_1] < \bar{y} < y_2 + \xi_0^{-1}[I_2(\xi_2) - y_2\xi_2] \quad (22)$$

where ξ_0, as before, is the scaled thickness number, y_u is the lower limit of y for infinite thickness, $\xi_1(y_1)$, in the infinite-case integration employing $[y_u, C(y_u)]$, is any particular ξ at which integration is stopped, y_2 and ξ_2 are the boundary y_0 and ξ_0 for the highest finite case available, and

$$I_2(\xi) \equiv \int_1^{y(\xi)} y \frac{d\xi}{dy} dy$$

The situation is depicted in Figure 5. The stated inequalities follow from the diagram, which is based on families of numerical concentration profiles, *cf.* Figures 2 and 3, since

$$\bar{y} = \frac{\int y d\xi}{\int d\xi}$$

and

$$I_2(\xi_1) + y_u(\xi_0 - \xi_1) < \int_1^{\xi_0} y d\xi < I_2(\xi_2) + y_2(\xi_0 - \xi_2) \quad (23)$$

Reactivity Ratio Determinations by Sequence Distribution Measurements

N. W. Johnston

Union Carbide Corporation, Research and Development, Bound Brook, New Jersey 08805.
Received April 2, 1970

ABSTRACT: A relationship was developed for finding copolymer reactivity ratios using only one copolymer rather than a series of copolymers as is done in conventional approaches. This approach relates the comonomer feed, the copolymer composition, and the copolymer sequence distribution to reactivity ratios. Experimental evidence is shown that accurate measurements of the copolymer sequence distribution and the single copolymer reactivity ratio technique can be used to predict reactivity ratios that agree well with literature values obtained by standard techniques.

There are several standard methods for finding copolymer reactivity ratios. Approaches such as the Fineman–Ross[1] or Mayo–Lewis[2] relationships require preparation of a series of copolymers from various monomer feed compositions. The reactivity ratios for the series are then found by a graphical technique.

In preparing new copolymers, or when working with difficult-to-obtain monomers, it would be advantageous to be able to find copolymer reactivity ratios without the time and monomer consuming preparation of many samples. The use of copolymer sequence distribution statistical relationships and the development of advanced polymer analytical techniques for measuring sequence distributions now make this possible for some copolymer systems. Accurate measurement of the sequence distribution of one copolymer combined with the monomer feed and the copolymer composition can be used to give a pair of reactivity ratios. These reactivity ratios may then be used to predict the comonomer feed necessary to prepare a desired copolymer composition with a minimum investment of time and monomer.

Experimental Section

Preparation of Copolymers. Vinyl chloride–amyl methacrylate (VCl–AMA), vinyl chloride–hexyl methacrylate (VCl–HxMA), and vinyl chloride–heptyl methacrylate (VCl–HpMA) copolymers were prepared in 2-butanone at 40° from freshly distilled monomers which contained 0.4 wt % *t*-butyl peroxypivalate as initiator. Conversions were kept low and polymers were isolated by pouring the polymerization mixtures into a large excess of methanol. The polymers were reprecipitated several times from 2-butanone solutions by addition of the solutions to methanol. The samples were dried *in vacuo* and copolymer compositions were determined by C, H, Cl analysis.

Preparation of vinyl chloride–methyl methacrylate[3] (VCl–MMA), vinyl chloride–butyl methacrylate[4] (VCl–BMA),

(1) M. Fineman and S. D. Ross, *J. Polym. Sci.*, **5**, 259 (1950).
(2) F. R. Mayo and F. M. Lewis, *J. Amer. Chem. Soc.*, **66**, 1594 (1944).
(3) N. W. Johnston and H. J. Harwood, *J. Polym. Sci., Part C*, **22**, 591 (1969).
(4) N. W. Johnston, *Polym. Prepr., Amer. Chem. Soc., Div. Polym. Sci.*, **10** (2), 608 (1969).